

Transition from weak to strong measurements by nonlinear quantum feedback control

Jing Zhang,^{1,2,*} Yu-xi Liu,^{3,2} Re-Bing Wu,^{1,2} Chun-Wen Li,^{1,2} and Tzyh-Jong Tarn^{4,2}

¹Department of Automation, Tsinghua University, Beijing 100084, P. R. China

²Center for Quantum Information Science and Technology,

Tsinghua National Laboratory for Information Science and Technology, Beijing 100084, P. R. China

³Institute of Microelectronics, Tsinghua University, Beijing 100084, P. R. China

⁴Department of Electrical and Systems Engineering,
Washington University, St. Louis, MO 63130, USA

(Dated: March 26, 2019)

We find that feedback control may induce “pseudo” nonlinear dynamics in a damped harmonic oscillator, whose centroid trajectory in the phase space behaves like a classical nonlinear system. Thus, similar to nonlinear amplifiers (e.g., rf-driven Josephson junctions), feedback control on the harmonic oscillator can induce nonlinear bifurcation, which can be used to amplify small signals and further to measure quantum states of qubits. Using the circuit QED systems as an example, we show how to apply our method to measure superconducting charge qubits.

PACS numbers: 03.65.Sq, 03.65.Ta, 85.25.-j

I. INTRODUCTION

Quantum feedback control [1] is one of the central parts of quantum control theory and applications [2, 3, 4, 5] owing to its potential ability to improve the stability and robustness of the system. Besides the extensive theoretical studies [6, 7, 8, 9, 10], recent rapid developments on sensitive measurements and manipulation techniques in atom-optical [11, 12, 13] and solid-state systems [14] have made it possible to implement quantum feedback control in laboratories.

In atom-optical systems, atomic ensembles are put in optical cavities with high quality factors. The information of the states of the atomic ensembles can be extracted by the probe lights transmitted through the optical cavities. Photocurrents induced by the probe lights are processed by field programmable gate arrays to generate real-time control signals, which can be fed back to design the electromagnetic fields imposed on the atom ensembles [11]. Possible applications of quantum feedback control in such systems include state stabilization [15], entanglement production [16], spin squeezing [17], and state discrimination [12]. Similar studies can be found in solid-state systems [18], e.g., the superconducting circuit-QED systems [19], in which quantum feedback control has been proposed to cool and squeeze the motion of a nanomechanical resonator [20, 21, 22, 23]. In these studies, the position of the nanomechanical resonator can be measured by a single electron transistor [21] or a rf-SQUID [22, 24, 25].

Among the existing theoretical studies on quantum feedback control, most are concentrated on linear quantum systems, i.e., the dynamical equations of the system are linear equations in the Heisenberg picture and the feedback controls are linear as well, which can often be

reduced to standard classical control problems, e.g., the Linear Quadratic Gaussian control problem [8, 9]. However, essential differences arise when we study nonlinear quantum systems: (i) linear quantum systems possess evenly spaced discrete energy spectra, while the distributions of energy levels in nonlinear systems are uneven or continuous; (ii) the linear quantum system starting from a Gaussian state always stays in a Gaussian state during the evolution, while nonlinear quantum dynamics generally distorts the wavepacket. Moreover, the presence of the relaxation and dephasing effects in nonlinear quantum systems may give rise to inherent phenomena in nonlinear classical systems, e.g., chaos [26] and bifurcation [27]. These dissipation-induced nonlinear effects [26, 27] have various applications in laboratories. For example, nonlinear dynamical bifurcation of a rf-driven Josephson junction is used to amplify small signals [28], and further applied to the readouts of the superconducting qubit states in experiments [28, 29].

Here we propose a method to mimic nonlinear dynamics using a harmonic oscillator with the feedback control. Such a proposal can be applied to a wider range, especially for those implementations that a nonlinear amplifier like the rf-driven Josephson junction is not achievable. It should be noticed that the manipulation of nonlinear effects via feedback has been widely studied in classical systems [30]. However, to what extent can we apply this to quantum systems? In particular, an extensively discussed question is *whether or not the nonlinear effects [31] can be produced in linear quantum systems by quantum feedback control*. Here we first address this question by examining a damped harmonic oscillator that is driven by a nonlinear feedback control, and then we will discuss how to use this “pseudo” nonlinear amplifier to read out quantum states by an example.

Our proposal is motivated by the recent developments for the quantum state readouts in superconducting quantum circuits via a nonlinear amplifier [28] and the quantum information processing using the cavity QED effect

*Electronic address: jing-zhang@mail.tsinghua.edu.cn

(e.g., in atom-optical systems, cavity quantum-dot systems, and for the interaction between the superconducting qubits and the transmission line resonator). In contrast to the measurement of the quantum states using a nonlinear amplifier (e.g., to read out the states of a superconducting qubit using a rf-driven Josephson junction [28]), one merit for our study is that the dynamics of the qubit-resonator system can be analytically solved even in the “nonlinear” regime, which makes it possible to see how to control the rate of the information extraction so as to balance between the measurement sensitivity and the measurement-induced disturbance in the bifurcation readout regime. Our study can be applied to the measurement of the states of an atom inside a cavity, quantum dots interacting with single-mode cavity field, or superconducting qubits in the circuit QED systems. Without loss of generality, below we choose the circuit QED system as an example to demonstrate our method, because the circuit QED system is more experimentally controllable and developed very quickly in recent years. Thus our proposal might be more possible to be demonstrated in such system.

The paper is organized as follows: in Sec. II, we present our feedback control proposal by a general model in which a damped harmonic oscillator is measured by a homodyne detection and then driven by the output field of the feedback control loop. The model of a system, in which a transmission line resonator is dispersively coupled to a charge qubit and driven by an outer feedback control circuit, is discussed in Sec. III. The nonlinear dynamics, induced by quantum feedback control in the transmission line resonator, is studied in Sec. IV, and its application to the qubit readout is shown in Sec. V. The conclusions and discussions are given in Sec. VII.

II. CONTROLLED DAMPED HARMONIC OSCILLATOR

Let us first study a damped harmonic oscillator with an angular frequency ω and a damping rate γ . The system is driven by a control signal u_t , and the leakage of the harmonic oscillator is detected by a homodyne measurement with efficiency η . Under the weak measurement assumption [32], the dynamics of the harmonic oscillator with the state ρ and the measurement output dy for measuring the position operator x can be described by the stochastic equations [7, 8, 9, 10, 11]:

$$\begin{aligned} d\rho &= -\frac{i}{\hbar}[H, \rho]dt + \gamma\mathcal{D}[a]\rho dt + \sqrt{\eta\gamma}\mathcal{H}[a]\rho dW, \\ dy &= \langle x \rangle dt + \frac{1}{\sqrt{2\eta\gamma}}dW, \end{aligned} \quad (1)$$

where $\langle x \rangle = \text{tr}(x\rho)$ is the average of the position operator x ; a and a^\dagger are the annihilation and creation operators of the harmonic oscillator whose Hamiltonian is $H = \hbar\omega a^\dagger a + \hbar u_t x$. The term $\hbar u_t x$ represents the interaction between the harmonic oscillator and a time-

dependent classical control field characterized by u_t . The superoperators $\mathcal{D}[c]\rho$ and $\mathcal{H}[c]\rho$ are defined by:

$$\begin{aligned} \mathcal{D}[c]\rho &= c\rho c^\dagger - \frac{1}{2}(c^\dagger c\rho + \rho c^\dagger c), \\ \mathcal{H}[c]\rho &= c\rho + \rho c^\dagger - \text{tr}(c\rho + \rho c^\dagger)\rho. \end{aligned}$$

The measurement is performed over the position operator

$$x = \frac{1}{\sqrt{2}}(a + a^\dagger),$$

whose conjugate momentum operator is

$$p = \frac{i}{\sqrt{2}}(a^\dagger - a).$$

dW is a measurement-induced Wiener noise satisfying

$$E(dW) = 0, \quad (dW)^2 = dt$$

with $E(\cdot)$ representing the ensemble average over the stochastic noise.

As shown in Eq. (1), dW represents the measurement-induced noise in the measurement output of the homodyne detection. To reduce the influence of the noise in the feedback control design, we can average the output signal over a long-time period that is far larger than $1/\gamma$, and take

$$Y_t = \frac{1}{t} \int_0^t \left(\langle x \rangle d\tau + \frac{1}{\sqrt{2\eta\gamma}} dW \right) = \frac{1}{t} \int_0^t dy \quad (2)$$

as an estimation of the position x . When the state of the system given by Eq. (1) tends to a stationary state, the stochastic process $\{\langle x \rangle(t)\}$ can be looked as a stationary process for $t \gg 1/\gamma$. Recall that in the ergodic theory it is stated that the time-average of a stationary process equals to its ensemble average (see, e.g., Ref. [33]), thus we have

$$\lim_{t \rightarrow \infty} \left(\frac{\int_s^t dy}{t-s} - \bar{x} \right) = 0, \quad \bar{x} = E(\langle x \rangle),$$

when $s \gg 1/\gamma$. Furthermore, it can be calculated that

$$\begin{aligned} \lim_{t \rightarrow \infty} \frac{1}{t} \int_0^t dy &= \lim_{t \rightarrow \infty} \frac{\int_0^s dy}{t} + \lim_{t \rightarrow \infty} \frac{t-s}{t} \lim_{t \rightarrow \infty} \frac{\int_s^t dy}{t-s} \\ &= \lim_{t \rightarrow \infty} \frac{\int_s^t dy}{t-s}, \end{aligned}$$

then we have

$$\lim_{t \rightarrow \infty} (Y_t - \bar{x}) = 0,$$

i.e., the estimated position Y_t converges to the corresponding ensemble average for sufficiently long time. Taking the long-time average of the stochastic signals is an effective filtering strategy to extract stationary signals from the background noises, and the time-average

signal, e.g., Y_t in Eq. (2), can be further used to design feedback control. Such a control design has been used in the literature to prepare desired quantum states (see, e.g., Ref. [34] for the Dicke state preparation).

With these considerations, we choose an arbitrary control function $f(\cdot)$, and let

$$u_t = -f(Y_t), \quad (3)$$

then we have $u_t \rightarrow -f(\bar{x})$ when $t \gg 1/\gamma$.

As a feedback control, the control given by Eq. (3) can be applied to the original system (1). If the initial state of the harmonic oscillator is a coherent state

$$|\alpha_0\rangle = \left| \frac{1}{\sqrt{2}}(x_0 + ip_0) \right\rangle,$$

then the state at time t approaches to the following coherent state:

$$|\bar{\alpha}\rangle = \left| \frac{1}{\sqrt{2}}(\bar{x} + i\bar{p}) \right\rangle,$$

when $t \gg 1/\gamma$, where \bar{x} and \bar{p} obey the following equations (see Appendix A):

$$\begin{aligned} \dot{\bar{x}} &= -\frac{\gamma}{2}\bar{x} + \omega\bar{p}, & \bar{x}(t_0) &= x_0, \\ \dot{\bar{p}} &= -\omega\bar{x} + f(\bar{x}) - \frac{\gamma}{2}\bar{p}, & \bar{p}(t_0) &= p_0. \end{aligned} \quad (4)$$

The above equations characterize the long-time behavior of the centroid trajectory of the system given by Eqs. (1) and (3). The nonlinear dynamics is present when the function $f(\bar{x})$ in Eq. (4) contains second-order or higher-order monomials of \bar{x} . Here, in order to facilitate our discussions, it is assumed that the solution of Eq. (4) tends to a time-independent stationary state $(x^*, p^*)^T$ in sufficiently long time.

The above analyses show that the first-order quadratures $\langle x \rangle$ and $\langle p \rangle$ of the controlled system evolve nonlinearly for $t \gg 1/\gamma$, while the evolutions of higher-order quadratures coincide with those of linear quantum systems in which coherent states remain to be coherent states. Therefore, the nonlinear dynamics induced by the proposed quantum feedback control is somewhat “semiclassical” (see the simplified diagram of the feedback control circuit in Fig. 1), in contrast with the dynamics of the system governed by a fully quantum nonlinear Hamiltonian in which the Gaussian wavepackets are distorted. For this reason, we call this feedback-control-induced nonlinear dynamics as “pseudo” nonlinear dynamics. As shown below, interesting phenomena can be observed when such a “pseudo” nonlinear system is coupled to another quantum system. That is, similar to the nonlinear amplifier using the nonlinear dynamical bifurcation (e.g., rf-driven Josephson junctions [28]), the harmonic oscillator with feedback control can be used to amplify small signals, and furthermore read out the qubit states.

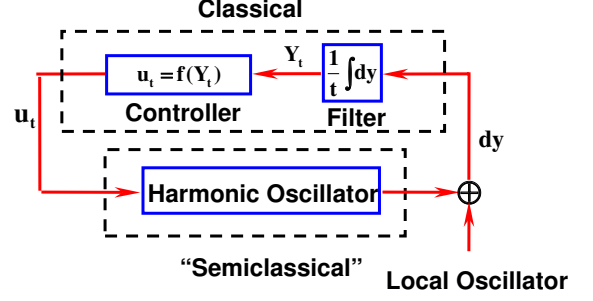


FIG. 1: (Color online) Simplified diagram of the feedback control circuit: the harmonic oscillator is measured by a homodyne detection, and the output signal of the homodyne measurement is fed into a classical control circuit which is composed of an integral filter and a controller. The output signal of the control circuit is further fed back to drive the harmonic oscillator, and this feedback control signal may induce nonlinear dynamics of the harmonic oscillator.

III. QUBIT-RESONATOR COUPLING

To demonstrate how we can use the “pseudo” nonlinear oscillator produced by feedback control to measure qubit states, let us consider an example. As shown in Fig. 2, a transmission line resonator is capacitively coupled to a Cooper pair box (charge qubit). The Hamiltonian of the coupled qubit-resonator system driven by a microwave with angular frequency ω_d can be expressed as [35]:

$$\begin{aligned} H &= \frac{\hbar\omega_q}{2}\sigma_z + \hbar\omega_T a^\dagger a + \hbar g(a^\dagger\sigma_- + a\sigma_+) \\ &\quad + \hbar u_t \frac{1}{\sqrt{2}}(a^\dagger e^{-i\omega_d t} + a e^{i\omega_d t}), \end{aligned} \quad (5)$$

where ω_q and ω_T are the angular frequencies of the charge qubit and the electric field in the transmission line resonator; σ_z and σ_\pm are the Pauli operator and ladder operators of the charge qubit; a and a^\dagger are the annihilation and creation operators of the single-mode electric field in the transmission line resonator; g is the qubit-resonator coupling strength; and u_t is the coupling constant between the driving field and the transmission line resonator.

In the dispersive regime, i.e., $|\Delta| = |\omega_q - \omega_T| \gg |g|$, we can apply the following unitary transformation

$$U = \exp \left[\frac{g}{\Delta} (a\sigma^\dagger - a^\dagger\sigma_-) \right]$$

to the Hamiltonian H in Eq. (5), then we have

$$\begin{aligned} \tilde{H} = U H U^\dagger &\approx \frac{\hbar(\omega_q + \chi)}{2}\sigma_z + \hbar\omega_T a^\dagger a + \hbar\chi a^\dagger a \sigma_z \\ &\quad + \hbar u_t \frac{1}{\sqrt{2}}(a^\dagger e^{-i\omega_d t} + a e^{i\omega_d t}). \end{aligned} \quad (6)$$

Furthermore, the Hamiltonian \tilde{H} can be rewritten in the rotating reference frame under the unitary transforma-

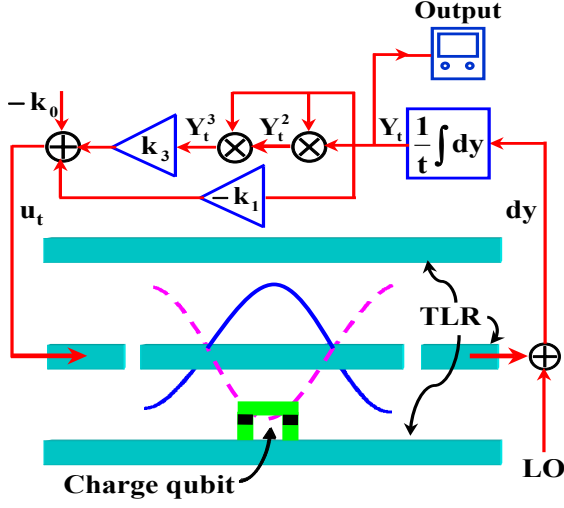


FIG. 2: (Color online) Schematic diagram of the superconducting circuit under feedback control. A charge qubit is capacitively coupled to a transmission line resonator (TLR), whose output field is detected by a homodyne measurement (“LO” denotes a local oscillator). The output signal of the homodyne measurement is fed into an electric control circuit to generate the desired control signal, which is further used to drive the electric field in the transmission line resonator.

tion

$$U_{\text{rot}} = \exp [i (\omega_d t) a^\dagger a],$$

thus we can obtain the following effective Hamiltonian

$$\begin{aligned} H_{\text{eff}} &= U_{\text{rot}} \tilde{H} U_{\text{rot}}^\dagger + i \dot{U}_{\text{rot}} U_{\text{rot}}^\dagger \\ &= \frac{\hbar \omega_q}{2} \sigma_z + \hbar \Delta_T a^\dagger a + \hbar \chi a^\dagger a \sigma_z + \hbar u_t x, \end{aligned} \quad (7)$$

where $\Delta_T = \omega_T - \omega_d$ is the angular frequency detuning between the electric field in the transmission line resonator and the driving field; $\chi = g^2/\Delta$ is the effective coupling strength between the charge qubit and the transmission line resonator; and $x = (a + a^\dagger)/\sqrt{2}$ is the position operator. Here the frequency-shift of the charge qubit caused by the interaction has been neglected under the condition that $\omega_q \gg \chi$.

It should be pointed out that higher-order nonlinear terms of a and a^\dagger can be introduced if we expand the effective Hamiltonian in Eq. (6) to higher-order terms of g/Δ . In fact, if we expand the Hamiltonian in Eq. (6) to $(g/\Delta)^3$ terms, we can obtain the following effective Hamiltonian:

$$\begin{aligned} \tilde{H}_{\text{eff}} &= \frac{\hbar}{2} \left(\omega_q + \frac{g^2}{\Delta} + \frac{g^4}{2\Delta^3} \right) \sigma_z + \hbar \omega_T a^\dagger a \\ &\quad + \hbar \frac{g^2}{\Delta} a^\dagger a \sigma_z - \hbar \frac{g^4}{\Delta^3} (a^\dagger a)^2 \sigma_z. \end{aligned} \quad (8)$$

The last term in Eq. (8) may induce nonlinear dynamics of the electric field in the transmission line resonator.

However, this term is $(g/\Delta)^2$ times smaller than the last second term in Eq. (8), and thus is too small to be observed in the large-detuning regime $g \ll \Delta$. In fact, with the experimentally realizable parameters adopted in the succeeding discussions, this high-order nonlinear term can be omitted compared with the linear terms and the nonlinear terms introduced by the quantum feedback control proposed below.

IV. FEEDBACK-CONTROL-INDUCED “NONLINEAR” DYNAMICS

As shown in Fig. 2, the leakage of the electric field in the transmission line resonator is detected by a homodyne measurement. We assume that the evolution of the qubit-resonator system is conditioned on the measurement output of the homodyne detection. Thus, this evolution can be described by the stochastic master equation given in Eq. (1) by replacing the system Hamiltonian H in Eq. (1) by H_{eff} given in Eq. (7). The output signal of the homodyne detection is integrated to obtain a new output signal $Y_t = \int_0^t dy/t$, which is further fed into a nonlinear amplification circuit to produce the following control signal:

$$u_t = -k_1 Y_t + k_3 Y_t^3 - k_0, \quad (9)$$

where the positive numbers k_0, k_1, k_3 are the control parameters. In the following discussions, the control parameters k_1 and k_3 will be chosen such that $k_1 > \gamma, k_3 > 0$. We will show that such a simple third-order nonlinear feedback control induces a static bifurcation that can be used to enhance the measurement strength for the qubit readout.

Different from the open-loop control that is predetermined by the designer without any information extraction, the proposed feedback control u_t is automatically adjusted according to the state of the charge qubit in real time so that different controls generate different state trajectories and thus different output signals. This makes it possible to identify the state of the charge qubit by amplifying the difference between the output signals by the designed control. This feature of feedback control has been reported in the literature to enhance the measurement intensity by linear amplification (see, e.g., Ref. [36]), which can be done more efficiently via nonlinear amplification induced by the proposed quantum feedback control.

Assume that the qubit-resonator system is initially in a separable state

$$\rho(0) = \rho_q(0) \otimes |\alpha_0\rangle\langle\alpha_0|,$$

where

$$\rho_q(0) = \sum_{i,j=g,e} \rho_{ij}(0) |i\rangle\langle j|$$

is the initial state of the charge qubit with ground state $|g\rangle$ and excited state $|e\rangle$, and $|\alpha_0\rangle$ is a coherent state of

the transmission line resonator with an amplitude $\alpha_0 = x_0/\sqrt{2}$, then the state of the qubit-resonator system at time $t \gg 1/\gamma$ can be expressed as [35]:

$$\rho(t) = \sum_{i,j=g,e} \rho_{ij}(t) |i\rangle\langle j| \otimes |\alpha_i(t)\rangle\langle\alpha_j(t)|, \quad (10)$$

where both $|\alpha_e(t)\rangle$ and $|\alpha_g(t)\rangle$ are coherent states. Let

$$\alpha_{g,e} = \frac{1}{\sqrt{2}}(x_{g,e} + ip_{g,e}),$$

then $x_{g,e}$ and $p_{g,e}$ evolve as below (see the deviations in the Appendix A):

$$\begin{aligned} \dot{x}_{g,e} &= -\frac{\gamma}{2}x_{g,e} + (\Delta_T \mp \chi)p_{g,e}, \\ \dot{p}_{g,e} &= -\frac{\gamma}{2}p_{g,e} - (\Delta_T \mp \chi - k_1)x_{g,e} - k_3x_{g,e}^3 + k_0, \end{aligned} \quad (11)$$

with the initial conditions: $x_{g,e}(0) = x_0$, $p_{g,e}(0) = 0$. The coefficients $\rho_{ij}(t)$ in Eq. (10) are given by:

$$\begin{aligned} \rho_{gg}(t) &= \rho_{gg}(0), \quad \rho_{ee}(t) = \rho_{ee}(0), \quad \rho_{ge}(t) = \rho_{eg}^*(t), \\ \rho_{eg}(t) &= \frac{\exp[-\gamma_2 t - i(\omega_q t + 2\chi \int_0^t \alpha_e(s)\alpha_g^*(s)ds)]}{\langle\alpha_g(t)|\alpha_e(t)\rangle} \rho_{eg}(0), \end{aligned}$$

where γ_2 is the dephasing rate of the charge qubit without measurement.

As analyzed in the last paragraph of Sec. II, the transmission line resonator can be looked as a “semiclassical” pseudo nonlinear system driven by an outer classical feedback control circuit (see the simplified version of the feedback control circuit in Fig. 3). The interaction between such a pseudo nonlinear system and the qubit brings two aspects of effects. On the one hand, for the qubit, this interaction brings additional decoherence. In fact, it can be calculated that there exists a measurement-induced dephasing factor $e^{-\Gamma(t)}$ for the reduced states of the charge qubit with

$$\Gamma(t) = \chi \int_0^t [x_e(s)p_g(s) - p_e(s)x_g(s)] ds. \quad (12)$$

On the other hand, this interaction leads to additional frequency shift for the transmission line resonator depending on the state of the charge qubit. Therefore it is possible to dispersively read out the states of the charge qubit under appropriate conditions.

We should emphasize at the end of this section that the nonlinear dynamics introduced by our feedback control proposal is quite different from the one induced by a nonlinear Hamiltonian (about x and p) such as:

$$H_{nl} = \frac{1}{2}p^2 + \frac{1}{2}\omega^2 x^2 - kx^4, \quad (13)$$

which may be obtained by higher-order perturbation expansion (see the last paragraph in Sec. III) or induced by an extra quantum bifurcation amplifier, e.g., a rf-driven

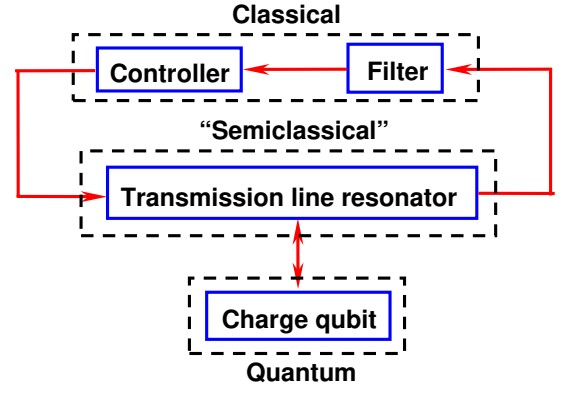


FIG. 3: (Color online) Simplified version for the feedback control circuit of the coupled qubit-resonator system as shown in Fig. 2: the charge qubit is coupled to the transmission line resonator, which is driven by a feedback control circuit composed of a filter and a controller. The nonlinear feedback control coming from the control circuit leads to “semiclassical” nonlinear dynamics of the electric field in the transmission line resonator. The static bifurcation induced by such nonlinear dynamics can be used to amplify small signals and thus measure the charge qubit.

Josephson junction as shown in Ref. [28]. Here the subscript “nl” means that the Hamiltonian contains high-order nonlinear terms. In our feedback control proposal, we introduce nonlinear terms like $\langle x \rangle^3$ to the dynamical equation of the system in comparison to the terms $\langle x^3 \rangle$ introduced by the nonlinear Hamiltonian H_{nl} in Eq. (13). With this difference, under the nonlinear Hamiltonian H_{nl} , the equations of the first order quadratures $\langle x \rangle$, $\langle p \rangle$ and the second order quadratures V_x , V_p and C_{xp} like Eq. (A1) are not closed. Higher-order quadratures such as $\langle x^3 \rangle$ should be considered. Even under the Gaussian assumption, i.e., the state of the system remains to be a Gaussian state if the initial state is a Gaussian state, the equations of $\langle x \rangle$, $\langle p \rangle$ and V_x , V_p , C_{xp} are coupled nonlinear equations, which cannot be analytically solved. However, in our proposal, the equations of $\langle x \rangle$, $\langle p \rangle$ and V_x , V_p , C_{xp} are decoupled if the initial state of the transmission line resonator is a coherent state (see the analysis in the Appendix A), which makes it possible to obtain the analytical stationary solution of the dynamical equation and control the information extraction rate shown in Eq. (12) by adjusting tunable parameters.

V. BIFURCATION-INDUCED QUANTUM MEASUREMENT

Equation (11) can be rewritten as the following nonlinear equation:

$$\begin{aligned} \dot{x} &= -\frac{\gamma}{2}x + \tilde{\omega}p, \\ \dot{p} &= -(\tilde{\omega} - k_1)x - k_3x^3 - \frac{\gamma}{2}p + k_0, \end{aligned} \quad (14)$$

where $\tilde{\omega} = \Delta_T \mp \chi$. Here the subscripts “e” and “g” adopted in Eq. (11) have been neglected, because the corresponding equations for the two cases are in the same form as in Eq. (14). A static pitchfork bifurcation occurs at a critical angular frequency

$$\tilde{\omega}^* = \frac{1}{2} \left(k_1 - \sqrt{k_1^2 - \gamma^2} \right). \quad (15)$$

When $\tilde{\omega} < \tilde{\omega}^*$, the system given by Eq. (14) possesses only one stable equilibrium, which becomes unstable when $\tilde{\omega} > \tilde{\omega}^*$ and, in the meanwhile, two other stable equilibria appear.

Therefore, by tuning the angular frequency ω_d of the driving field near the bifurcation point, the static bifurcation introduced by the proposed feedback control can induce a transition from weak to strong measurements for the qubit readout. Actually, let us first assign

$$\omega_d = \omega_T - \Delta_T^* + 2\chi, \quad (16)$$

where

$$\Delta_T^* = \frac{1}{2} \left(k_1 - \sqrt{k_1^2 - \gamma^2} \right)$$

is the bifurcation angular frequency. When $t \gg 1/\gamma$, the measurement outputs corresponding to the two eigenstates of the charge qubit are

$$Y_{g,e}(t) \sim x_{g,e}^\infty = k_0 \frac{\Delta_{g,e}}{(\Delta_{g,e})^2 - k_1 \Delta_{g,e} + \gamma^2/4} \quad (17)$$

respectively. Both effective angular frequencies $\Delta_g = \Delta_T^* - 3\chi$ and $\Delta_e = \Delta_T^* - \chi$ corresponding to the two eigenstates of the charge qubit are lower than Δ_T^* . If k_0 is small enough such that

$$k_0 \ll \left| \frac{\chi^2 - 2\chi\Delta_T^* + k_1\chi}{\Delta_T^* - \chi} \right|, \quad (18)$$

both $Y_g(t)$ and $Y_e(t)$ are so close to zero that they are almost indistinguishable. When $t \gg 1/\gamma$, we have

$$\begin{aligned} x_{g,e} &\sim x_{g,e}^\infty = \frac{k_0 \Delta_{g,e}}{\Delta_{g,e}^2 - k_1 \Delta_{g,e} + \frac{\gamma^2}{4}}, \\ p_{g,e} &\sim p_{g,e}^\infty = \frac{\gamma}{2\Delta_{g,e}} x_{g,e}^\infty, \end{aligned}$$

then we can calculate the measurement-induced dephasing rate Γ_{weak} from Eq. (12) and obtain

$$\begin{aligned} \Gamma(t) &\sim \chi (x_e^\infty p_g^\infty - p_e^\infty x_g^\infty) t \\ &= \frac{\gamma \chi k_0^2 (\Delta_e - \Delta_g)/2}{\prod_{i=g,e} \left(\Delta_i^2 - k_1 \Delta_i + \frac{\gamma^2}{4} \right)} t = \Gamma_{\text{weak}} t, \end{aligned}$$

or equivalently

$$\Gamma_{\text{weak}} = \frac{\gamma k_0^2 \chi^2}{\left[(\Delta_g)^2 - k_1 \Delta_g + \frac{\gamma^2}{4} \right] \left[(\Delta_e)^2 - k_1 \Delta_e + \frac{\gamma^2}{4} \right]}. \quad (19)$$

The tiny separation between $Y_g(t)$ and $Y_e(t)$ can be amplified by switching the angular frequency of the driving field from $\omega_d = \omega_T - \Delta_T^* + 2\chi$ to $\tilde{\omega}_d = \omega_T - \Delta_T^*$. When $t \gg 1/\gamma$, the corresponding stationary measurement outputs are

$$\begin{aligned} Y_g(t) &\sim \tilde{x}_g^\infty = k_0 \frac{\tilde{\Delta}_g}{\tilde{\Delta}_g^2 - k_1 \tilde{\Delta}_g + \frac{\gamma^2}{4}}, \\ Y_e(t) &\sim \tilde{x}_e^\infty = \sqrt{\frac{-\tilde{\Delta}_e^2 + k_1 \tilde{\Delta}_e - \gamma^2/4}{k_3 \tilde{\Delta}_e}}. \end{aligned} \quad (20)$$

Under this condition, the two effective angular frequencies $\tilde{\Delta}_g = \Delta_T^* - \chi$ and $\tilde{\Delta}_e = \Delta_T^* + \chi$ are lower and higher than the bifurcation angular frequency Δ_T^* respectively. By setting

$$k_3 \ll \left| \frac{\chi^2 + 2\chi\Delta_T^* - k_1\chi}{\Delta_T^* + \chi} \right|, \quad (21)$$

we have

$$|\tilde{x}_e^\infty - \tilde{x}_g^\infty| \gg |x_e^\infty - x_g^\infty|.$$

The above result means that the difference between the two output signals corresponding to the two eigenstates of the charge qubit is amplified by the proposed nonlinear feedback control. When $t \gg 1/\gamma$, it can be calculated that

$$\begin{aligned} x_g &\sim \tilde{x}_g^\infty = k_0 \frac{\tilde{\Delta}_g}{\tilde{\Delta}_g^2 - k_1 \tilde{\Delta}_g + \frac{\gamma^2}{4}}, \\ x_e &\sim \tilde{x}_e^\infty = \sqrt{\frac{-\tilde{\Delta}_e^2 + k_1 \tilde{\Delta}_e - \gamma^2/4}{k_3 \tilde{\Delta}_e}}, \\ p_g &\sim \tilde{p}_g^\infty = \frac{\gamma}{2\tilde{\Delta}_g} \tilde{x}_g^\infty, \\ p_e &\sim \tilde{p}_e^\infty = \frac{\gamma}{2\tilde{\Delta}_e} \tilde{x}_e^\infty. \end{aligned}$$

Then, we can obtain the measurement-induced dephasing rate Γ_{strong} from Eq. (12) as

$$\begin{aligned} \Gamma(t) &\sim \chi (\tilde{x}_e^\infty \tilde{p}_g^\infty - \tilde{p}_e^\infty \tilde{x}_g^\infty) t \\ &= \frac{k_0 \gamma \chi^2 t}{\sqrt{k_3 \tilde{\Delta}_e^3}} \cdot \frac{\sqrt{-\tilde{\Delta}_e^2 + k_1 \tilde{\Delta}_e - \gamma^2/4}}{\tilde{\Delta}_g^2 - k_1 \tilde{\Delta}_g + \gamma^2/4} = \Gamma_{\text{strong}} t, \end{aligned}$$

or equivalently

$$\Gamma_{\text{strong}} = \frac{k_0 \gamma \chi^2}{\sqrt{k_3 \tilde{\Delta}_e^3}} \cdot \frac{\sqrt{-\tilde{\Delta}_e^2 + k_1 \tilde{\Delta}_e - \gamma^2/4}}{\tilde{\Delta}_g^2 - k_1 \tilde{\Delta}_g + \gamma^2/4}. \quad (22)$$

It can be noticed that Γ_{strong} is far greater than Γ_{weak} when k_0 and k_3 are sufficiently small to satisfy Eqs. (18) and (21).

VI. NUMERICAL SIMULATIONS

Let us now discuss experimental feasibility via the numerical simulation using the experimentally accessible parameters. According to the current experiments (see, e.g., Ref. [19]), the qubit frequency ω_q , the frequency ω_T and the decay rate γ of the transmission line resonator, as well as the coupling constant g between the qubit and the transmission line resonator can be chosen as,

$$\begin{aligned} \omega_q/2\pi &= 5.1 \text{ GHz}, & \omega_T/2\pi &= 5 \text{ GHz}, \\ \gamma/2\pi &= 100 \text{ MHz}, & g/2\pi &= 20 \text{ MHz}. \end{aligned} \quad (23)$$

With the conditions given in Eqs (18) and (21), we further assume that the parameters k_0 , k_1 , and k_3 are

$$\begin{aligned} k_0/2\pi &= 20 \text{ MHz}, \\ k_1/2\pi &= 200 \text{ MHz}, \\ k_3/2\pi &= 2 \text{ MHz or } 10 \text{ MHz}. \end{aligned} \quad (24)$$

The frequency $\omega_d/2\pi$ of the driving field is initially chosen to be 4.995 GHz. At the time $t^*/\tau = 100$, i.e., $t^* = 50$ ns, the frequency $\omega_d/2\pi$ of the driving field is switched from 4.995 GHz to 4.987 GHz, where $\tau = 0.5$ ns is a normalization time scale. Simulation results in Fig. 4 show that, at time t^* , the difference between the two output signals $Y_g(t)$ and $Y_e(t)$, i.e., the measurement sensitivity, suddenly jumps. The measurement-induced dephasing rate also suddenly jumps from Γ_{weak} to Γ_{strong} . In fact, it can be calculated from Eqs. (19) and (22) that $\Gamma_{\text{weak}}/2\pi \approx 0.36$ MHz and $\Gamma_{\text{strong}}/2\pi \approx 10.22$ MHz (or 4.57 MHz) when $k_3/2\pi = 2$ MHz (or 10 MHz). This indicates that the static bifurcation introduced by our proposal induces a transition from weak to strong measurements at time t^* . Moreover, as shown in Eq. (20) and the simulation results in Fig. 4, the decrease of the nonlinear coefficient k_3 makes the measurement more sensitive, but accelerates the dephasing of the qubit. *Such a tradeoff between measurement sensitivity and measurement-induced dephasing effects is a natural consequence of the confliction between information extraction and measurement-induced disturbance, which is inherent for quantum measurement.*

VII. CONCLUSION

In summary, we present a method to induce “semiclassical” nonlinear dynamics in a damped harmonic oscillator by quantum feedback control. We use the coupled qubit-resonator system as a concrete example to demonstrate our proposal. We assume that a nonlinear feedback control is applied to a coupled qubit-resonator system to induce a static bifurcation, which is used to amplify the small frequency-shift of the transmission line resonator for the qubit readout. Theoretical analysis and numerical simulations show an evident transition from weak to strong measurements near the bifurcation point. Our

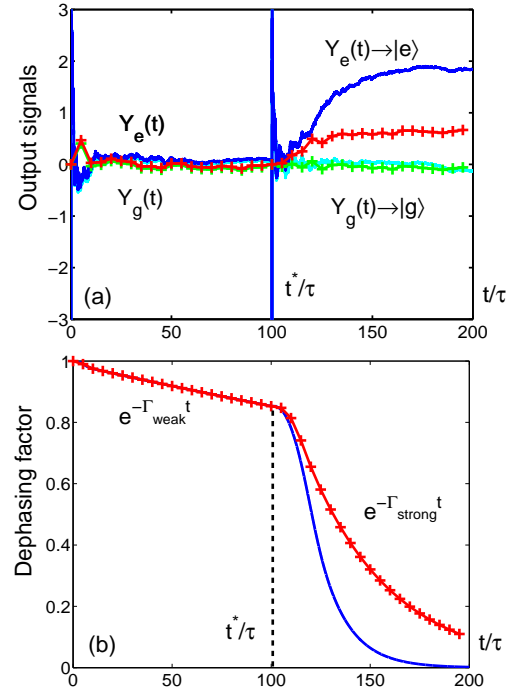


FIG. 4: (Color online) Bifurcation-induced transition from a weak measurement to a strong measurement with (a) the two output signals $Y_g(t)$ and $Y_e(t)$ corresponding to the two eigenstates $|g\rangle$ and $|e\rangle$ of the charge qubit, and (b) the measurement-induced dephasing factor. The parameter $\tau = 0.5$ ns is the normalization time scale. The solid curves represent the trajectories with a nonlinear coefficient $k_3/2\pi = 2$ MHz, while the solid curves with plus signs represent the trajectories with $k_3/2\pi = 10$ MHz.

proposal works as well as the bifurcation readout proposal by a nonlinear amplifier, e.g., a rf-driven Josephson junction. Additionally, we can tune the information extraction rate to balance between information extraction and measurement-induced disturbance in the “nonlinear” readout regime.

We emphasize that the proposed cavity-assistant nonlinear amplification strategy can also be applied to the qubit readouts in other experimental implementations, such as cavity QED or quantum dot-cavity systems. All analyses on the measurements have no difference with those for the discussed coupled qubit-resonator system. This generalized result is important because the nonlinear amplification device, like the rf-driven Josephson junctions in superconducting circuits, may not be achievable, thus the proposed measurement method, using feedback control induced nonlinear amplification, might be more efficient.

Our study is also hopeful to be extended to quantum demolition measurements, e.g., the detection of momentum or position of a nanomechanical resonator, for which the measurement-induced back-action effects on the quantity being measured cannot be neglected.

ACKNOWLEDGMENTS

We acknowledge financial support from the National Natural Science Foundation of China under Grant Nos. 60704017, 60904034, 60635040, 60674039. Y. X. Liu is supported by the National Natural Science Foundation of China under No. 10975080. T. J. Tarn would also like to acknowledge partial support from the U. S. Army Research Office under Grant W911NF-04-1-0386.

APPENDIX A: SEMICLASSICAL DYNAMICS OF THE CONTROLLED HARMONIC OSCILLATOR

From the stochastic master equation (1) given in Sec. II, we can obtain the following equations for the expectations, variances of the position x and momentum p of the controlled harmonic oscillator and the covariance of x and p :

$$\begin{aligned} d\langle x \rangle &= -\frac{\gamma}{2}\langle x \rangle dt + \omega\langle p \rangle dt + \sqrt{2\eta\gamma}\left(V_x - \frac{1}{2}\right)dW, \\ d\langle p \rangle &= -\omega\langle x \rangle dt - \frac{\gamma}{2}\langle p \rangle dt - u_t dt + \sqrt{2\eta\gamma}C_{xp}dW, \\ \dot{V}_x &= -\gamma V_x + 2\omega C_{xp} + \frac{\gamma}{2} - 2\eta\gamma\left(V_x - \frac{1}{2}\right)^2, \\ \dot{V}_p &= -\kappa V_p - 2\omega C_{xp} + \frac{\gamma}{2} - 2\eta\gamma C_{xp}^2, \\ \dot{C}_{xp} &= -\gamma C_{xp} + \omega V_p - \omega V_x - 2\eta\gamma\left(V_x - \frac{1}{2}\right)C_{xp}, \end{aligned} \quad (\text{A1})$$

where the variances of the position x and momentum p are defined as:

$$V_x = \langle x^2 \rangle - \langle x \rangle^2, \quad V_p = \langle p^2 \rangle - \langle p \rangle^2,$$

and

$$C_{xp} = \left\langle \frac{xp + px}{2} \right\rangle - \langle x \rangle \langle p \rangle$$

is the symmetric covariance of the position x and momentum p . As shown in Eq. (A1), the evolutions of the variances V_x , V_p and the symmetric covariance C_{xp} can be described by deterministic equations which are totally decoupled from the evolutions of $\langle x \rangle$ and $\langle p \rangle$, and also from the control u_t . It can be derived for Gaussian states (see also Eqs. (48)-(50) in Ref. [37] and Eqs. (10) and (11) in Ref. [38]). Let us take V_x as an example. From the stochastic master equation (1), we have:

$$\begin{aligned} dV_x &= \left(-\gamma V_x + 2\omega C_{xp} + \frac{\gamma}{2} - 2\eta\gamma\left(V_x - \frac{1}{2}\right)^2 \right) dt \\ &\quad + \sqrt{2\eta\gamma}K_{xxx}dW, \end{aligned} \quad (\text{A2})$$

where

$$K_{xxx} = \left\langle (x - \langle x \rangle)^3 \right\rangle$$

is the third-order quadrature of x . Since the initial state of the harmonic oscillator is a Gaussian (coherent) state, high-order quadratures such as K_{xxx} vanish for this state. Further calculations show that the equations of these high-order quadratures are independent of the control u_t , and thus the dynamics of these high-order quadratures is the same as that of linear systems, which means that $K_{xxx}(t) \equiv 0, \forall t > 0$. Thus we know that the dW term in Eq. (A2) vanishes, which leads to the deterministic equation of the variance V_x given in Eq. (A1).

Additionally, since the harmonic oscillator is initially in a coherent state under which $V_x(0) = V_p(0) = 1/2$ and $C_{xp}(0) = 0$, it can be verified from Eq. (A1) that the state of the harmonic oscillator always stays in a coherent state during the course of the evolution, i.e., $V_x(t) = V_p(t) \equiv 1/2$ and $C_{xp}(t) \equiv 0, \forall t > 0$. Under this condition, the stochastic fluctuation terms corresponding to dW in the equations of $\langle x \rangle$ and $\langle p \rangle$ vanish. Thus, the stochastic equation (A1) can be reduced to

$$\begin{aligned} \dot{\langle x \rangle} &= -\frac{\gamma}{2}\langle x \rangle + \omega\langle p \rangle, \\ \dot{\langle p \rangle} &= -\omega\langle x \rangle - \frac{\gamma}{2}\langle p \rangle - u_t. \end{aligned} \quad (\text{A3})$$

Furthermore, from the ergodic theory [33], we have

$$u_t = -f(Y_t) \rightarrow -f(\bar{x})$$

when $t \gg 1/\gamma$, where

$$Y_t = \frac{1}{t} \int_0^t \left(\langle x \rangle d\tau + \frac{1}{\sqrt{2\eta\gamma}} dW \right)$$

and $\bar{x} = E(\langle x \rangle)$ is the ensemble average over the stochastic noise dW . Then, the long-time behavior of Eq. (A3) can be described by the following equations:

$$\begin{aligned} \dot{\bar{x}} &= -\frac{\gamma}{2}\bar{x} + \omega\bar{p}, \\ \dot{\bar{p}} &= -\omega\bar{x} + f(\bar{x}) - \frac{\gamma}{2}\bar{p}, \end{aligned}$$

which finishes our analysis.

-
- [1] H. M. Wiseman and G. J. Milburn, *Quantum Measurement and Control* (Cambridge University Press, Cambridge, 2009).
- [2] D. D'Alessandro, *Introduction to Quantum Control and Dynamics* (Chapman & Hall, Boca Raton, 2007).
- [3] H. Mabuchi and N. Khaneja, *Int. J. Robust Nonlinear Control* **15**, 647 (2005).
- [4] D. Y. Dong, I. R. Petersen, arXiv:0910.2350v1 [quant-ph].
- [5] N. Ganesan and T. J. Tarn, *Phys. Rev. A* **75**, 032323 (2007); D. Y. Dong, C. B. Zhang, H. Rabitz, A. Pechen, T. J. Tarn, *J. Chem. Phys.* **129**, 154103 (2008); W. Cui, Z. R. Xi, and Y. Pan, *Phys. Rev. A* **77**, 032117 (2008); M. Zhang, H. Y. Dai, Z. R. Xi, H. W. Xie, and D. W. Hu, *Phys. Rev. A* **76**, 042335 (2007).
- [6] V. P. Belavkin, *J. Multivariate Anal.* **42**, 171 (1992); V. P. Belavkin, *Commun. Math. Phys.* **146**, 611 (1992); V. P. Belavkin, *Theor. Probab. Appl.* **38**, 573 (1993).
- [7] H. M. Wiseman and G. J. Milburn, *Phys. Rev. Lett.* **70**, 548 (1993); H. M. Wiseman and G. J. Milburn, *Phys. Rev. A* **47**, 642 (1993).
- [8] A. C. Doherty, S. Habib, K. Jacobs, H. Mabuchi, and S. M. Tan, *Phys. Rev. A* **62**, 012105 (2000).
- [9] M. R. James, H. I. Nurdin, and I. R. Petersen, *IEEE Trans. Automat. Contr.* **53**, 1787 (2008); J. E. Gough, *Phys. Rev. A* **78**, 052311 (2008); N. Yamamoto, *Phys. Rev. A* **74**, 032107 (2006).
- [10] R. Ruskov and A. N. Korotkov, *Phys. Rev. B* **66**, 041401(R) (2002); L. Bouten, R. van Handel, and M. R. James, *SIAM J. Control Optim.* **46**, 2199 (2007); L. Bouten, M. Guta, H. Maassen, *J. Phys. A: Math. Gen.* **37**, 3189 (2004).
- [11] H. Mabuchi and A. C. Doherty, *Science* **298**, 1372 (2002).
- [12] R. L. Cook, P. J. Martin, and J. M. Geremia, *Nature* **446**, 774 (2007).
- [13] G. G. Gillett, R. B. Dalton, B. P. Lanyon, M. P. Almeida, M. Barbieri, G. J. Pryde, J. L. O'Brien, K. J. Resch, S. D. Bartlett, A. G. White, arXiv:0911.3698v1 [quant-ph].
- [14] J. Q. You and F. Nori, *Physics Today* **58** (11), 42 (2005); Y. Makhlin, G. Schön, and A. Shnirman, *Rev. Mod. Phys.* **73**, 357 (2001); J. Clarke and F. K. Wilhelm, *Nature* **453**, 1031 (2008); A. A. Clerk, M. H. Devoret, S. M. Girvin, F. Marquardt, and R. J. Schoelkopf, arXiv:0810.4729v1 [cond-mat.mes-hall].
- [15] R. van Handel, J. K. Stockton, and H. Mabuchi, *IEEE Trans. Automat. Contr.* **50**, 768 (2005); H. F. Hofmann, G. Mahler, and O. Hess, *Phys. Rev. A* **57**, 4877 (1998); J. Wang and H. M. Wiseman, *Phys. Rev. A* **64**, 063810 (2001); X. S. Liu, W. Z. Liu, R. B. Wu, and G. L. Long, *J. Opt. B: Quantum Semiclass. Opt.* **7**, 66 (2005); H. M. Wiseman, S. Mancini, and J. Wang, *Phys. Rev. A* **66**, 013807 (2002).
- [16] S. Mancini and H. M. Wiseman, *Phys. Rev. A* **75**, 012330 (2007); C. Hill and J. Ralph, *Phys. Rev. A* **77**, 014305 (2008); A.R.R. Carvalho and J. J. Hope, *Phys. Rev. A* **76**, 010301 (2007); S. Mancini and J. Wang, *Eur. Phys. J. D*, **32**, 257 (2005).
- [17] L. K. Thomsen, S. Mancini, and H. M. Wiseman, *Phys. Rev. A* **65**, 061801 (2002).
- [18] P. Zhang, Y. D. Wang, and C. P. Sun, *Phys. Rev. Lett.* **95**, 097204 (2005); J. Q. You, Y. X. Liu, and F. Nori, *Phys. Rev. Lett.* **100**, 047001 (2008); M. Grajcar, S. Ashhab, J. R. Johansson, and F. Nori, *Phys. Rev. B* **78**, 035406 (2008); Y. D. Wang, Y. Li, F. Xue, C. Bruder, and K. Semba, *Phys. Rev. B* **80**, 144508 (2009); F. Xue, Y. D. Wang, Y. X. Liu, and F. Nori, *Phys. Rev. B* **76**, 205302 (2007); N. Lambert and F. Nori, *Phys. Rev. B* **78**, 214302 (2008); S. H. Ouyang, J. Q. You, and F. Nori, *Phys. Rev. B* **79**, 075304 (2009).
- [19] A. Blais, R. S. Huang, A. Wallraff, S. M. Girvin and R. J. Schoelkopf, *Phys. Rev. A* **69**, 062320 (2004); A. Wallraff, D. I. Schuster, A. Blais, L. Frunzio, R.-S. Huang, J. Majer, S. Kumar, S. M. Girvin and R. J. Schoelkopf, *Nature* **431**, 162 (2004).
- [20] R. Ruskov, K. Schwab, and A. N. Korotkov, *Phys. Rev. B* **71**, 235407 (2005).
- [21] A. Hopkins, K. Jacobs, S. Habib, and K. C. Schwab, *Phys. Rev. B* **68**, 235328 (2003).
- [22] J. Zhang, Y. X. Liu, and F. Nori, *Phys. Rev. A* **79**, 052102 (2009).
- [23] K. Jähne, C. Genes, K. Hammerer, M. Wallquist, E. S. Polzik, and P. Zoller, *Phys. Rev. A* **79**, 063819 (2009); Ya. S. Greenberg, E. Il'ichev, F. Nori, arXiv:0906.5420v2 [cond-mat.mes-hall].
- [24] M. P. Blencowe and E. Buks, *Phys. Rev. B* **76**, 014511 (2007); E. Buks and M. P. Blencowe, *Phys. Rev. B* **74**, 174504 (2006); E. Buks, S. Zaitsev, E. Segev, B. Abdo, and M. P. Blencowe, *Phys. Rev. E* **76**, 026217 (2007).
- [25] S. Etaki, M. Poot, I. Mahboob, K. Onomitsu, H. Yamaguchi, and H.S.J. van der Zant, *Nature Phys.* **4**, 785 (2008).
- [26] T. Bhattacharya, S. Habib, and K. Jacobs, *Phys. Rev. Lett.* **85**, 4852 (2000); S. Habib, K. Jacobs, and K. Shizume, *Phys. Rev. Lett.* **96**, 010403 (2006).
- [27] M. A. Armen and H. Mabuchi, *Phys. Rev. A* **73**, 063801 (2006).
- [28] I. Siddiqi, R. Vijay, F. Pierre, C. M. Wilson, M. Metcalfe, C. Rigetti, L. Frunzio, and M. H. Devoret, *Phys. Rev. Lett.* **93**, 207002 (2004); I. Siddiqi, R. Vijay, M. Metcalfe, E. Boaknin, L. Frunzio, R. J. Schoelkopf, and M. H. Devoret, *Phys. Rev. B* **73**, 054510 (2006).
- [29] A. Lupascu, C. J. M. Verwijs, R. N. Schouten, C. J. P. M. Harmans, and J. E. Mooij, *Phys. Rev. Lett.* **93**, 177006 (2004); A. Lupascu, E. F. C. Driessen, L. Roschier, C. J. P. M. Harmans, and J. E. Mooij, *Phys. Rev. Lett.* **96**, 127003 (2006); A. Lupascu, S. Saito, T. Picot, P. C. de Groot, C. J. P. M. Harmans and J. E. Mooij, *Nat. Phys.* **3**, 119 (2007).
- [30] A. Isidori, *Nonlinear Control Systems*, 3rd edition, (Springer Verlag, London, 1995).
- [31] K. Jacobs and A. P. Lund, *Phys. Rev. Lett.* **99**, 020501 (2007).
- [32] S. Ashhab, J. Q. You, and F. Nori, *Phys. Rev. A* **79**, 032317 (2009); S. Ashhab, J. Q. You, and F. Nori, *New J. Phys.* **11**, 083017 (2009); S. Ashhab, J. Q. You, Franco Nori, arXiv:0903.2319v1 [quant-ph].
- [33] K. Petersen, *Ergodic Theory (Cambridge Studies in Advanced Mathematics)* (Cambridge University Press, Cambridge, 1990).
- [34] J. K. Stockton, R. vanHandel, and H. Mabuchi, *Phys. Rev. A* **70**, 022106 (2004).
- [35] J. Gambetta, A. Blais, M. Boissonneault, A. A. Houck,

- D. I. Schuster, and S. M. Girvin, Phys. Rev. A **77**, 012112 (2008); D. WahyuUtami and A. A. Clerk, Phys. Rev. A **78**, 042323 (2008).
- [36] J. Combes, H. M. Wiseman, and K. Jacobs, Phys. Rev. Lett. **100**, 160503 (2008).
- [37] A. C. Doherty and K. Jacobs, Phys. Rev. A, **60**, 2700 (1999).
- [38] H. M. Wiseman and A. C. Doherty, Phys. Rev. Lett., **94**, 070405 (2005).